

New Permanent Magnets and New Processing Techniques

J. Wecker, S. Schultz, M. Katter, D. Schnitzke, and C. Kuhrt

Since the discovery of $\text{Nd}_2\text{Fe}_{14}\text{B}$ in 1984, a number of new phases with uniaxial anisotropy like $\text{Sm}(\text{Fe},\text{X})_{12}$, $\text{Sm}_5(\text{Fe},\text{Ti})_{17}$, $(\text{Sm},\text{Zr})\text{Fe}_3$, and $\text{Sm}_2\text{Fe}_{17}\text{N}_3$ have been investigated. Their intrinsic magnetic properties compare favorably with $\text{Nd}_2\text{Fe}_{14}\text{B}$. Magnetic hardening is possible by rapid quenching or mechanical alloying, which both result in isotropic materials with coercivities of up to 51 kA/cm. Mechanical alloying is a new technique to prepare high-performance permanent magnets at low temperatures. For Nd-Fe-B, isotropic and anisotropic magnets with properties comparable to sintered or melt spun materials can be produced.

1 Introduction

THE energy product of permanent magnets has continuously improved since the beginning of this century (Fig. 1). This mainly results from two developments—first from the optimization of the alloy composition and the further development of the processing techniques for a given material, and second from the discovery of new classes of materials (like Sm-Co or, recently, Nd-Fe-B). Currently, the production of rare earth (RE) based magnets relies on conventional powder metallurgy, *i.e.*, sintering.^[1] Only for Nd-Fe-B, the rapid solidification process provides an alternative route to high-performance magnets.^[2] In 1986, it was shown for the first time that Nd-Fe-B based materials with properties similar to melt spun ribbons can be obtained by mechanical alloying.^[3] Since then, this new process has been continuously improved and the properties of these magnets now are fully comparable to sintered or rapidly solidified materials.^[4] Simultaneously, new intermetallic phases with intrinsic properties comparable to $\text{Nd}_2\text{Fe}_{14}\text{B}$ have been found. Basically, these are Sm-Fe-X alloys, where X is necessary either to stabilize a new crystal structure, like in $\text{Sm}(\text{Fe},\text{X})_{12}$ [5-7] and $\text{Sm}_5(\text{Fe},\text{Ti})_{17}$ [8] or is needed to modify the magnetic anisotropy of a given structure, like in $(\text{Sm},\text{Zr})\text{Fe}_3$,^[9] $\text{Sm}_2\text{Fe}_{17}\text{N}_3$, and $\text{Sm}_2\text{Fe}_{17}\text{C}_x$.^[10,11]

It is the aim of this contribution to summarize the principles of the mechanical alloying process and its applicability to new alloy systems. Additionally, the intrinsic magnetic properties of the new phases will be recalled and compared to $\text{Nd}_2\text{Fe}_{14}\text{B}$. Their magnetic hardening by nonequilibrium techniques (*i.e.*, by rapid solidification and mechanical alloying) will be described and the advantages and disadvantages will be discussed by comparison with conventional sintering.

2 Mechanical Alloying of RE-Fe-X Alloys

Mechanical alloying originally was introduced as a method to prepare oxide-dispersion-strengthened (ODS) alloys,^[12] *i.e.*, microstructures difficult or impossible to prepare by conventional metallurgy. It circumvents many of the limitations of

conventional alloying of metals or metal/nonmetal components, which requires melting and thus is restricted to the phase diagram of the alloy system. Instead, mechanical alloying uses an interdiffusion reaction at low temperatures, which is enabled by the formation of ultrafine composite particles during milling in a high-energy ball mill. The powder particles are trapped by the colliding balls, become heavily deformed and cold welded, leading to characteristically layered particles. Additional milling refines the microstructure further and results in an intimate mixing of the elements on a nanometer scale. Depending on the thermodynamics of the alloy system, on the mechanical workability of the starting powders, and on the milling parameters, the interdiffusion reaction to form the alloy or intermetallic phases can either take place during milling or during a subsequent heat treatment.

Examples for mechanically alloyed materials are high-strength superalloys, oxide-dispersion-strengthened aluminum alloys, and intermetallic phases. Also, metastable phases have been produced by this process, including amorphous and quasi-crystalline alloys.^[13]

Mechanical alloying of RE-Fe-X (X = Ti, Mo, V, or Zr) powders is performed in a planetary ball mill under argon atmosphere. The elemental powders (Fe, X: 5 to 40 μm ; RE < 0.5 mm)

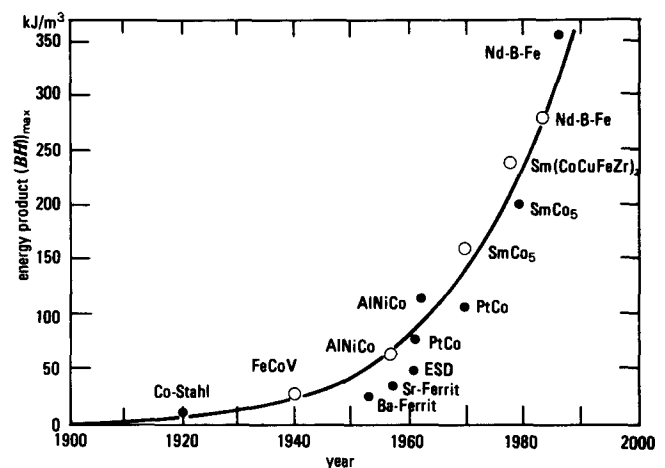


Fig. 1 Increase in energy product, $(BH)_{\text{max}}$, with time.

J. Wecker, L. Schultz, M. Katter, K. Schnitzke, and C. Kuhrt, Siemens AG, Research Laboratory, Erlangen, Germany.

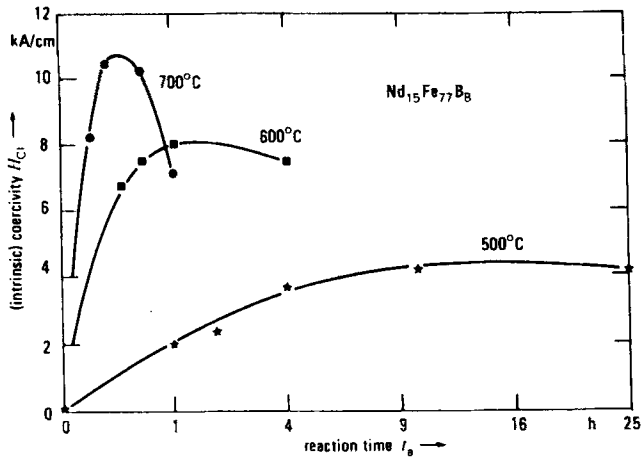


Fig. 2 Coercivity, H_{Ci} , of mechanically alloyed Nd-Fe-B as a function of annealing time, t_a .

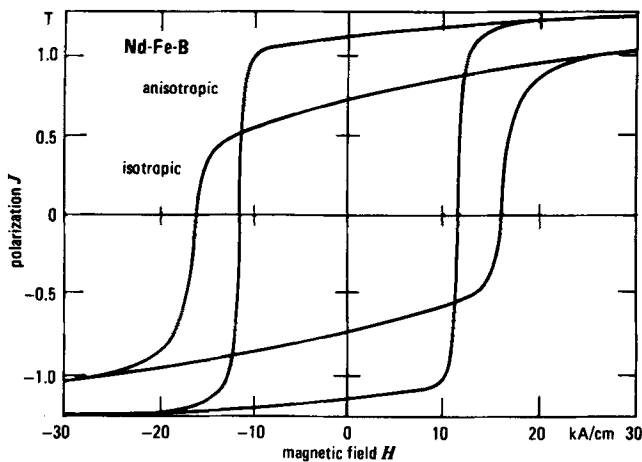


Fig. 4 Hysteresis loops of fully dense isotropic and anisotropic Nd-Fe-B prepared from mechanically alloyed precursors.

are mixed and poured into a cylindrical milling container with 10-mm diameter steel balls. The powder mixture is milled typically for 60 hr and the temperature of the powder particles during the collision of the balls is estimated to be about 300 to 400 °C. Generally, the microstructure that is established during milling depends on the milling parameters and on the thermodynamics of the alloy system. For Nd-Fe-B, layered Nd-Fe particles with embedded B are observed, and the layer thickness depends on the total milling time.^[3] In the case of alloy systems like Sm-Fe or Sm-Co, which have a negative ΔG (ΔG is the difference between the free enthalpy of the amorphous phase (which is regarded as an undercooled liquid) and the layered composite), an amorphous phase or a two-phase microstructure of an amorphous matrix and the Fe or Co solid solution is formed in a solid-state reaction *in situ* during milling. A negative ΔG favors the amorphous phase compared with the layered structure of the components.

The hard magnetic intermetallic phase is formed during a solid-state reaction after milling. The annealing temperatures

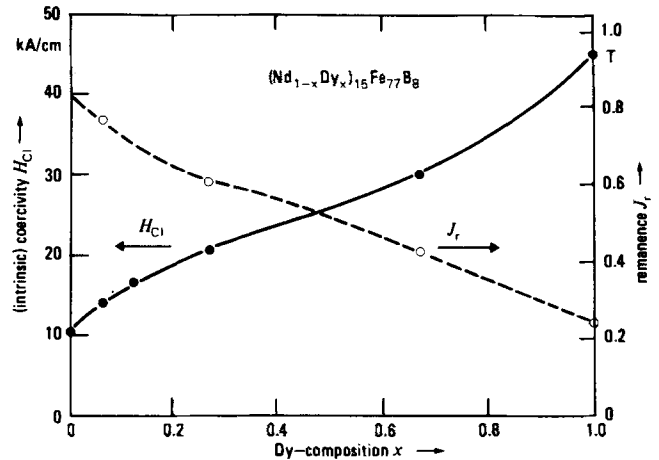


Fig. 3 Coercivity, H_{Ci} , and remanence, J_r , versus Dy content, x , in mechanically alloyed Nd-Dy-Fe-B powders.

can be as low as 500 °C, which enables the formation of a fine-grained microstructure. Too high temperatures or too long annealing times lead to excessive grain growth accompanied by a decrease in the coercivity (Fig. 2). For Nd-Fe-B, the properties of mechanically alloyed and rapidly quenched materials are very similar. High coercivities require off-stoichiometric (Nd-rich) compositions and a further increase is possible by substituting Dy for Nd, which results in higher anisotropy fields (Fig. 3). There is one major difference between the two techniques: Co-additions, which are known to increase the Curie temperature, result in a reduction in the coercivity for sintered magnets as well as for mechanically alloyed powder. Only melt spun ribbons quenched at intermediate wheel velocities directly into the crystalline state behave differently and exhibit the same coercivity as the Co-free material even at Co substitutions of 50%.^[14]

The mechanically alloyed powder is magnetically isotropic and can be processed to resin-bonded magnets. Alternatively, by hot pressing at temperatures around 700 °C, one obtains fully dense magnets. For high-energy products, $(BH)_{max}$, it is necessary to produce anisotropic magnets. This can be done by a subsequent deformation at the same temperature, which results in an anisotropic grain growth and a texture with the c -direction (and thus the direction of easy magnetization) parallel to the press direction. The process called die upsetting was developed by Lee for melt spun ribbons^[15] and was successfully adopted to mechanically alloyed powder. Figure 4 shows the hysteresis loops of fully dense isotropic and anisotropic Nd-Fe-B prepared from mechanically alloyed precursors. For the anisotropic magnet, the energy product is 250 kJ/m³ and the coercivity is 11.5 kA/cm. Higher $(BH)_{max}$ values require higher Fe concentrations, but lead to lower H_{Ci} and vice versa. Further optimization can be achieved by alloying with Co, Dy, etc.^[3]

3 New Phases

Since the discovery of Nd₂Fe₁₄B in 1984, a number of new phases with uniaxial anisotropy like Sm(Fe,X)₁₂, Sm₅(Fe,Ti)₁₇,

Table 1 Intrinsic Magnetic Properties of New Sm-Fe-X Phases

Alloy	Structure	Curie temperature (T_C), °C	H_a , kA/cm	J_s , T	$(BH)_{max}$, kJ/m ³
Sm(Fe,Ti) ₁₂	Tetragonal	320	80	1.10	240
Sm ₅ (Fe,Ti) ₁₇	Hexagonal	305	>160	0.90	160
(Sm,Zr)Fe ₃	Rhombohedral	385	110	0.90	160
Sm ₂ Fe ₁₇ N ₃	Rhombohedral	470	168	1.54	475
Nd ₂ Fe ₁₄ B	Tetragonal	315	60	1.60	512

Note: The maximum energy product, $(BH)_{max}$, is calculated according to $J_s^2/4\mu_0$. For details see text.

Table 2 Coercivity, Remanence, and Curie Temperature of Mechanically Alloyed 1:12-Type Alloys

Composition	Coercivity (H_{ci}), kA/cm	Remanence (J_r), T	Curie temperature (T_C), °C
Sm ₁₀ Fe ₈₀ Ti ₁₀	3.5	0.47	323
Sm ₁₀ Fe ₈₀ Mo ₁₀	3.8	0.47	232
Sm ₁₀ Fe ₈₀ V ₁₀	5.6	0.52	360
Sm ₁₂ Fe ₈₃ V ₁₅	8.6	0.46	327
Sm ₁₅ Fe ₇₀ V ₁₅	9.4	0.40	309

(Sm,Zr)Fe₃, and Sm₂Fe₁₇N₃ were found. All have significantly higher anisotropy fields, H_a , than Nd₂Fe₁₄B and a Curie temperature, T_C , which is at least comparable (Table 1). Their main disadvantage is the lower saturation polarization, J_s , which limits the maximum energy product $(BH)_{max} = J_s^2/4\mu_0$. Only the recently discovered interstitial Sm₂Fe₁₇ nitride has a high J_s value and thus, from a technical point of view, is the most interesting compound. However, because of the high H_a values, all phases have the potential for high coercivities, H_{ci} . In the following, the properties of the different systems will be summarized with the main focus on Sm₂Fe₁₇N_x.

3.1 Sm(Fe,X)₁₂

The iron-rich, rare earth-containing compounds RE(Fe,X)₁₂ were independently investigated by Buschow,^[5] Ohashi,^[6] and Müller.^[7] X denotes an additional element (e.g., Ti, V, Mo, or Si) needed to stabilize the tetragonal ThMn₁₂ crystal structure, which does not form in the binary RE-Fe alloys. As for Nd₂Fe₁₄B, <001> is the axis of easy magnetization for most rare earth elements. For the light RE, only the Sm compounds have a high H_a at room temperature, and therefore, high coercivities, H_{ci} , are only expected in Sm-Fe-X alloys.

In general, magnetic hardening of the 1:12 phases is difficult for two reasons. First, the ThMn₁₂ phases have a considerable homogeneity range, and the primary magnetic properties strongly depend on the composition,^[7] which is completely different to the line compound Nd₂Fe₁₄B. This makes it rather difficult to optimize the coercive properties, because both the microstructure of the alloy and the stoichiometry of the ThMn₁₂ phase have to be optimized, which cannot be done independently. Second, Sm(Fe,Ti)₁₂ either decomposes peritectically below about 800 °C into Sm₂(Fe,Ti)₁₇ and Fe₂Ti^[16] or at least it requires a strict control of the alloy composition, be-

cause the phase equilibria only enable the formation of 1:12 at Sm-poor concentrations.^[17] These difficulties may explain why no significant H_{ci} values have been achieved by conventional sintering techniques.

Despite of this, Sm(Fe,Ti)₁₂ can be formed (possibly in a metastable state) from mechanically alloyed powders or overquenched ribbons by a heat treatment at 700 °C. This is similar to SmCo₅, which crystallizes from an amorphous phase below its decomposition temperature.^[18] The alloy composition has to be off stoichiometric to obtain reasonable coercivities. In mechanically alloyed isotropic Sm₁₀Fe₈₀X₁₀ powders, the authors obtained H_{ci} values of 3.5 kA/cm, 3.8 kA/cm, and 5.6 kA/cm for X = Mo, Ti and V, respectively (Table 2). For the Sm-Fe-V system, the coercivity can be increased further to 9.4 kA/cm by increasing the Sm content to 15 at.%.^[19] This is linked to the occurrence of SmFe₂ at the grain boundaries of the matrix phase. Similar coercivities have been obtained in Sm(Fe,V)₁₂ by rapid quenching.^[20] Because both techniques result in magnetically isotropic samples, the remanence is restricted to $J_s/2$. The presence of secondary phases further dilutes the polarization, and thus, J_r typically is between 0.4 and 0.6 Tesla (T). An improvement is possible by substituting Co for Fe. This is known to increase the saturation polarization for the 1:12 phases,^[6,7] which can be understood within the rigid band model. Because the coercivity is not affected by Co additions, the remanence can be increased by up to 16%.^[21]

3.2 Sm₅(Fe,Ti)₁₇

Contrary to Sm-Fe-V, an increase of the Sm content destabilizes the ThMn₁₂ structure in the Sm-Fe-Ti system, and at Sm concentrations of about 16 at.%, a new phase forms, which so far has only been observed in thin films.^[22] The crystal structure of this phase is hexagonal, with $a = 2.014$ nm and $c = 1.233$ nm, and seems to be very similar to the A2 Nd₅Fe₁₇ phase recently found in the Nd-Fe system.^[23] The magnetic anisotropy field of Sm₅(Fe,Ti)₁₇ can be roughly estimated to more than 160 kA/cm, and the magnetization remains uniaxial up to the Curie temperature of 305 °C.^[24] The A2 phase has a complex unit cell with 264 atoms (e.g., 12 formula units)^[25] and a very sluggish formation kinetic. Thus, it is easily formed in thin films and by annealing a mechanically alloyed or rapidly quenched precursor,^[8,24,26] and it is only observed by chance in sintered Sm-Fe-Ti samples at grain boundaries where it possibly forms from SmFe₂ and Fe₂Ti.^[16] Sm₅(Fe,Ti)₁₇ decomposes

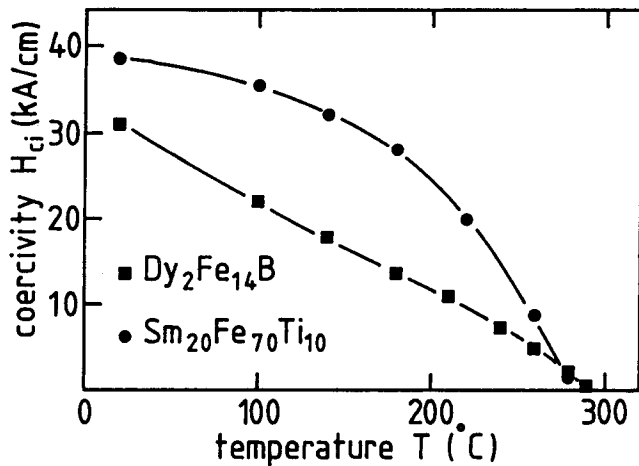


Fig. 5 Temperature dependence of the coercivity, H_{ci} , of melt spun Dy-Fe-B and Sm-Fe-Ti.

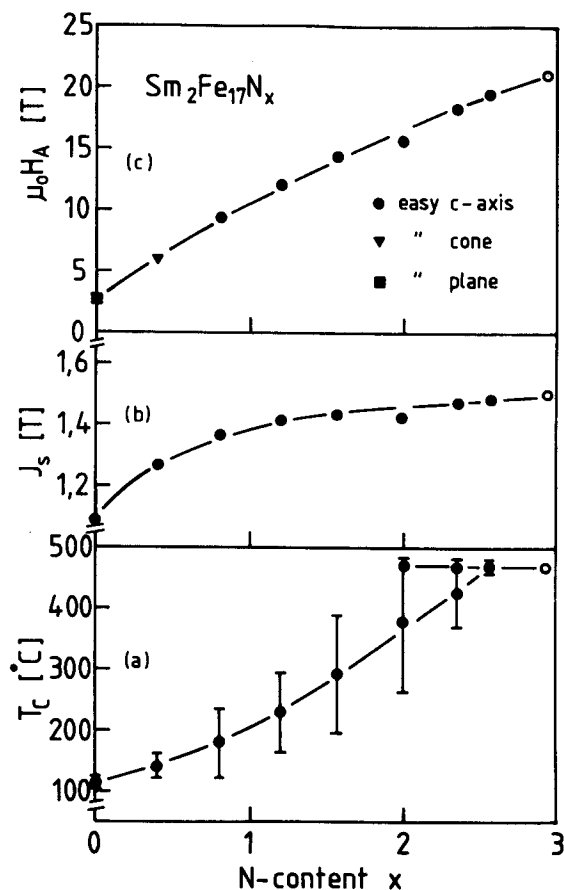


Fig. 6 Anisotropy field, H_a , saturation polarization, J_s , and Curie temperature, T_C , of $\text{Sm}_2\text{Fe}_{17}\text{N}_x$ versus N content, x .

above 800 °C, making it impossible to prepare bulk magnets by conventional sintering.

Isotropic $\text{Sm}_{26}\text{Fe}_{64}\text{Ti}_{10}$ powders prepared by mechanical alloying exhibit large coercivities of 51 kA/cm, but only a small remanence of 0.23 T. Lower Sm contents result in a lower coer-

Table 3 Anisotropy Field and Coercivities of Mechanically Alloyed and Rapidly Solidified Sm-Zr-Fe Alloys that Crystallize in the PuNi_3 Structure

Composition	Anisotropy (H_a), kA/cm	Coercivities (H_{ci}), kA/cm	
		Mechanically alloyed	Rapidly solidified
$\text{Sm}_{25}\text{Fe}_{75}$	110	8.4	...
$\text{Sm}_{20}\text{Zr}_7\text{Fe}_{73}$	100	10.4	10.2
$\text{Sm}_{17}\text{Zr}_{10}\text{Fe}_{73}$	84	10.2	6.0
$\text{Sm}_{14}\text{Zr}_{13}\text{Fe}_{73}$	64	6.8	2.7
$\text{Sm}_{11}\text{Zr}_{16}\text{Fe}_{73}$	4.6	...

civity, but a higher remanence.^[26] Again, high H_{ci} values require an off-stoichiometric composition, with the secondary phases being nonmagnetic at room temperature (as Fe_2Ti). Although it is in principle possible, the preparation of the $\text{Sm}_5(\text{Fe,Ti})_{17}$ phase by rapid quenching is complicated by the difficulty in suppressing the formation of $\text{Sm}(\text{Fe,Ti})_{12}$ and SmFe_2 during solidification.^[24] Both phases result in a constricted hysteresis loop because of their lower anisotropy compared to $\text{Sm}_5(\text{Fe,Ti})_{17}$.

Because of its great coercivity at room temperature, the coercivity of $\text{Sm}_5(\text{Fe,Ti})_{17}$ samples at elevated temperatures even is higher than that of (stoichiometric) $\text{Dy}_2\text{Fe}_{14}\text{B}$ (Fig. 5). It is of interest that the $H_{ci}(T)$ curve for the two materials has a different curvature, which probably results from a different temperature dependence of the anisotropy field of the A2 phase compared to $\text{Dy}_2\text{Fe}_{14}\text{B}$.

3.3 ($\text{Sm,Zr})\text{Fe}_3$

In the Sm-Fe-Zr system, neither the 1:12 nor the A2 phase is observed. Instead, the SmFe_3 phase forms with the rhombohedral PuNi_3 crystal structure, which consists of an alternate stacking of three RETM_5 (CaCu₅-type) and three RE_2TM_4 (Laves phase-type) layers (RE = rare earth element, TM = transition metal). This phase has a uniaxial magnetic anisotropy with an anisotropy field, H_a , of 110 kA/cm compared to 60 kA/cm for $\text{Nd}_2\text{Fe}_{14}\text{B}$ (Table 1). Zirconium additions enter on Sm lattice sites leading to a decrease of H_a due to the dilution of the Sm sublattice. The Curie temperature, which is mainly determined by the Fe-Fe exchange interaction, remains almost constant at 385 °C.^[9]

Although the SmFe_3 phase has been known for a long time, its high uniaxial anisotropy has only recently been recognized. Magnetic hardening is possible by mechanical alloying, resulting in a coercive field of 8.4 kA/cm (Table 3). Higher coercivities can be obtained for off-stoichiometric compositions and by an alloying with Zr (e.g., 10.4 kA/cm for $\text{Sm}_{20}\text{Zr}_7\text{Fe}_{73}$). For low Zr concentrations, the reduced anisotropy seems to be compensated for by a more favorably microstructure. Only at higher Zr contents does the decreasing anisotropy field also reduce the coercivity. Melt spun alloys often have $\text{Sm}_2\text{Fe}_{17}$ and SmFe_2 precipitates with a low magnetocrystalline anisotropy and thus reduced coercivities compared to mechanically alloyed samples. The best Sm-Zr-Fe materials have properties similar to those of 1:12-type Sm-Fe-V (Table 2). Early results

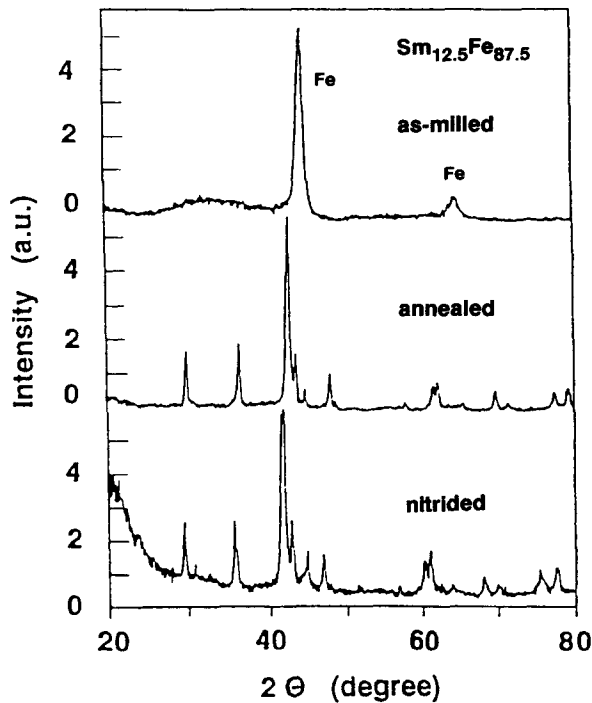


Fig. 7 X-ray diffraction patterns of Sm-Fe powder after mechanical alloying, annealing, and nitrogenation (from top to bottom).

on melt spun $\text{Sm}_{40}\text{Fe}_{60}$ ribbons^[27] yield coercivities of up to 19.2 kA/cm, which probably also resulted from the presence of the SmFe_3 phase.

3.4 $\text{Sm}_2\text{Fe}_{17}\text{N}_3$

As first shown by Coey and co-workers,^[10] $\text{Sm}_2\text{Fe}_{17}$ dissolves up to three nitrogen atoms per formula unit without changing the parent $\text{Th}_2\text{Zn}_{17}$ structure. The nitrogenation expands the lattice by up to 7%, which increases the Curie temperature to 480 °C, the saturation polarization to 1.54 T and, most importantly, induces a uniaxial magnetic anisotropy with an anisotropy field of 170 kA/cm.^[28] Thus, contrary to the phases discussed so far, $\text{Sm}_2\text{Fe}_{17}\text{N}_x$ is competitive with $\text{Nd}_2\text{Fe}_{14}\text{B}$ in all intrinsic magnetic properties. To ensure optimum magnetic properties, an almost complete nitrogenation is necessary, *i.e.*, x has to be between 2.5 and 3. With lower nitrogen contents ($x < 2.5$), one only obtains significantly reduced magnetic properties (Fig. 6), and below $x = 0.55$, the direction of easy magnetization changes from uniaxial to easy cone.

The complete substitution of Nd for Sm, as well as of Co for Fe, is possible without changing the $\text{Th}_2\text{Zn}_{17}$ structure, *i.e.*, one obtains a complete series of solid solutions.^[29,30] For $(\text{Sm}_{1-x}\text{Nd}_x)\text{Fe}_{17}\text{N}_y$, the magnetic anisotropy is significantly reduced with increasing x , and it changes from easy axis to easy cone at about $x = 0.6$ and to easy plane at about $x = 0.7$. Cobalt additions to $\text{Sm}_2(\text{Fe}_{1-x}\text{Co}_x)\text{Fe}_{17}\text{N}_y$ lead to an overall improvement in the magnetic properties, with H_a , J_s , and T_C showing maxima between $x = 0.2$ and $x = 0.5$. For Co-rich

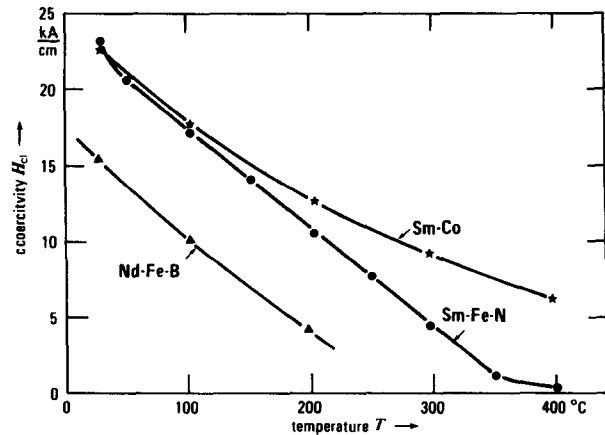


Fig. 8 Temperature dependence of the coercivity, H_{ci} , of mechanically alloyed isotropic $\text{Nd}_2\text{Fe}_{14}\text{B}$, SmCo_5 , and $\text{Sm}_2\text{Fe}_{17}\text{N}_x$ -type materials.

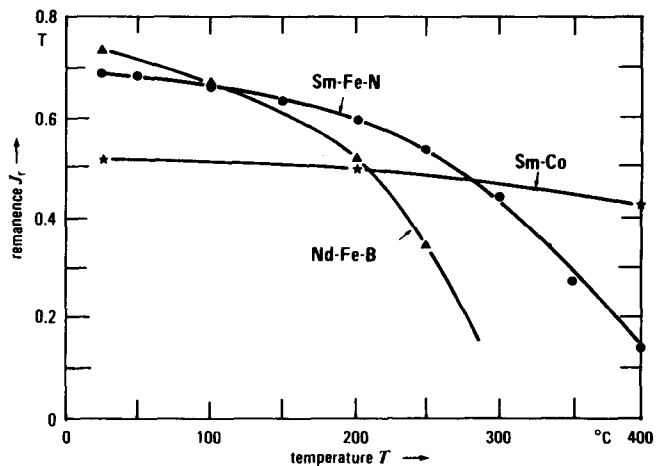


Fig. 9 Temperature dependence of the remanence, J_r , of mechanically alloyed isotropic $\text{Nd}_2\text{Fe}_{14}\text{B}$, SmCo_5 , and $\text{Sm}_2\text{Fe}_{17}\text{N}_x$ -type materials.

$\text{Sm}_2(\text{Fe}_{1-x}\text{Co}_x)_{17}$, the nitrogenation reduces the Curie temperature because of the reduction of TM-TM nearest neighbors with increasing nitrogen content.^[29]

The interstitial nitrides are prepared by a gas-solid reaction at temperatures typically between 400 and 500 °C. At higher temperatures, $\text{Sm}_2\text{Fe}_{17}\text{N}_3$ decomposes into SmN and $\alpha\text{-Fe}$. Because this reaction is irreversible, the $\text{Sm}_2\text{Fe}_{17}$ nitride is a metastable phase, and the decomposition occurs by the precipitation of $\alpha\text{-Fe}$ as soon as the temperature allows for the Fe diffusion. Any processing thus has to avoid temperatures above 500 °C after nitrogenation. In particular, the nitrogenation of bulk specimens is difficult because of the low diffusion coefficient of nitrogen in $\text{Sm}_2\text{Fe}_{17}$.^[31]

The authors succeeded in preparing isotropic $\text{Sm}_2\text{Fe}_{17}\text{N}_x$ powder with high coercivities of 24 kA/cm by mechanical alloying.^[32] The process includes first the preparation of an as-milled precursor, which is a two-phase mixture of an amorphous phase, and $\alpha\text{-Fe}$ (Fig. 7). A subsequent heat treatment between 700 and 750 °C leads to the formation of a fine-grained

Sm₂Fe₁₇ matrix phase. The following nitrogenation below 500 °C does not change the microstructure further and results in an isotropic hard magnetic powder with excellent properties at higher temperatures (Fig. 8 and 9), where Nd-Fe-B exhibits much poorer performance because of its lower Curie temperature. These powders can be processed to resin-bonded magnets and may substitute Nd-Fe-B or even Sm-Co for applications between 100 and 200 °C. A Zn-bonding at about 400 °C results in even higher H_{ci} values of up to 30 kA/cm, but decreases the remanence because of the Zn addition.^[33]

Like Sm₂Fe₁₇N_x, Sm₂Fe₁₇C_x also has the Th₂Zn₁₇ structure of binary Sm₂Fe₁₇, but with intrinsic properties that are somewhat smaller compared to the nitride. For the carbide, it is much more difficult to dissolve the maximum amount of C. Early attempts to prepare Sm₂Fe₁₇C_x by arc melting of Sm, Fe, and Fe₃C only led to $x = 1$.^[11] Recently, by gas phase carbonation of powders using hydrocarbon gases, Coey and co-workers obtained $x = 2$,^[34] with a significant improvement in the magnetic properties. Magnetic hardening is possible by mechanical alloying, with a somewhat lower coercivity of 18.5 kA/cm^[4] compared to Sm₂Fe₁₇N_x.

Rapid solidification of Sm-Fe alloys with compositions in the vicinity of Sm₂Fe₁₇ stabilizes the Th₂Zn₁₇ structure only at low quenching rates and high Sm concentrations.^[35] Otherwise, the hexagonal disordered TbCu₇ modification crystallizes. Because of the lower anisotropy of the nitrated TbCu₇ structure, nitrogenation of melt spun ribbons only results in high coercivities if the formation of the TbCu₇ phase is suppressed during solidification, or if it is transformed to the Th₂Zn₁₇ structure before the gas phase reaction. This and the occurrence of α -Fe precipitates make it much more difficult to obtain similar coercivities as through mechanical alloying. So far, optimum H_{ci} values for melt spun samples are 16.7 kA/cm.

4 Summary

Mechanical alloying is a new technique to prepare permanent magnets with properties that are similar to rapidly solidified materials. As a nonequilibrium technique, it circumvents many of the limitations of conventional sintering like the constrictions imposed by the phase diagram, *e.g.*, it enables the formation of (metastable) phases at low temperatures. A main advantage is the fact that the microstructure that is favorable for high coercivities, *i.e.*, grain sizes below the single domain particle diameter, is easily obtained. Here, a magnetically reversed grain is less detrimental than in sintered (nucleation-controlled) magnets that have grain sizes above 10 μm . Also, secondary phases are finely dispersed and probably impede the domain wall motion. This offers the chance for a quick evaluation of the potential inherent to new magnetic materials. A limitation of the nonequilibrium techniques is the fact that the preparation of anisotropic materials requires further processing steps, like hot deformation for Nd-Fe-B. Such techniques still have to be developed for the new materials.

The new phases not only provide the opportunity to obtain new insights into the magnetism of intermetallic compounds.

From a technical point of view, the excellent intrinsic magnetic properties of the interstitial nitrides make them competitive with Nd-Fe-B. At temperatures above 100 °C, the mechanically alloyed powders already exhibit superior coercive properties.

Acknowledgment

This work was supported by the German Ministry for Research and Technology and by the European Community in the framework of the Materials Research and EURAM/BRITE programs, respectively.

References

1. M. Sagawa, S. Fujimura, N. Togawa, H. Yamamoto, and Y. Matsumura, *J. Appl. Phys.*, **55**, 2083 (1984).
2. J.J. Croat, J.F. Herbst, R.W. Lee, and F.E. Pinkerton, *J. Appl. Phys.*, **55**, 2078 (1984).
3. L. Schultz, J. Wecker, and E. Hellstern, *J. Appl. Phys.*, **61**, 3583 (1987).
4. L. Schultz, K. Schnitzke, J. Wecker, M. Katter, and C. Kuhrt, *J. Appl. Phys.*, May (1992).
5. K.H.J. Buschow, Proc. 9th Int. Workshop on Rare-Earth Magnets and Their Applications, Bad Soden, Deutsche Physikalische Gesellschaft, Bad Honnef, 453 (1987).
6. K. Ohashi, T. Yokoyama, R. Osugi, and Y. Tawara, *IEEE Trans. Magn.*, **MAG-23**, 3101 (1987).
7. A. Müller, *J. Appl. Phys.*, **64**, 249 (1988).
8. K. Schnitzke, L. Schultz, J. Wecker, and M. Katter, *Appl. Phys. Lett.*, **56**, 587 (1990).
9. J. Wecker, M. Katter, K. Schnitzke, and L. Schultz, *J. Appl. Phys.*, **69**, 5847 (1991).
10. J.M.D. Coey and Hong Sun, *J. Magn. Magn. Mat.*, **87**, L251 (1990).
11. D.B. de Mooij and K.H.J. Buschow, *J. Less-Common Met.*, **142**, 349 (1988).
12. J.S. Benjamin, *Sci. Am.*, **234**, 40 (1976).
13. E. Arzt and L. Schultz, Ed., *New Materials by Mechanical Alloying Techniques*, DGM Informationsgesellschaft, Oberursel (1989).
14. J. Wecker and L. Schultz, *Appl. Phys. Lett.*, **51**, 697 (1987).
15. R.W. Lee, *Appl. Phys. Lett.*, **46**, 790 (1985).
16. W. Rodewald and P. Schrey, Proc. 6th International Symposium on Magnetic Anisotropy and Coercivity in Rare Earth-Transition Metal Alloys, S.G. Sankar, Ed., Carnegie Mellon University, Pittsburgh, 101, Oct (1990).
17. T.S. Jang and H.H. Stadelmaier, *J. Appl. Phys.*, **67**, 4957 (1990).
18. J. Wecker, M. Katter, and L. Schultz, *J. Appl. Phys.*, **69**, 6058 (1991).
19. L. Schultz, K. Schnitzke, and J. Wecker, *Appl. Phys., Lett.*, **56**, 868 (1990).
20. F.E. Pinkerton and D.J. VanWingerden, *IEEE Trans. Magn.*, **MAG-25**, 3306 (1989).
21. J. Wecker, M. Katter, K. Schnitzke, and L. Schultz, *J. Appl. Phys.*, **67**, 4951 (1990).
22. N. Kamprath, N.C. Liu, H. Hegde, and F.J. Cadieu, *J. Appl. Phys.*, **64**, 5720 (1988).
23. G. Schneider, F.J.G. Landgraf, V. Villas-Boas, G.H. Bezerra, F.P. Missell, and A.E. Ray, *Mater. Lett.*, **8**, 472 (1989).
24. M. Katter, J. Wecker, and L. Schultz, *IEEE Trans. Magn.*, **MAG-26**, 1379 (1990).
25. J.M. Moreau, L. Paccard, J.P. Nozieres, F.P. Missell, G. Schneider, and V. Villas-Boas, *J. Less-Common Met.*, **163**, 245 (1990).

26. L. Schultz, K. Schnitzke, J. Wecker, and M. Katter, *IEEE Trans. Magn.*, *MAG-26*, 1373 (1990).
27. J.J. Croat and J.F. Herbst, *J. Appl. Phys.*, *53*, 2404 (1982).
28. M. Katter, J. Wecker, and L. Schultz, *J. Appl. Phys.*, *70*, 3188 (1991).
29. M. Katter, J. Wecker, C. Kuhrt, L. Schultz, and R. Grössinger, *J. Magn. Mater.*, submitted for publication.
30. M. Katter, J. Wecker, C. Kuhrt, L. Schultz, X.C. Kou, and R. Grössinger, *J. Magn. Mater.*, submitted for publication.
31. J.M.D. Coey, J.F. Lawler, Hong Sun, and J.E.M. Allan, *J. Appl. Phys.*, *69*, 3007 (1991).
32. K. Schnitzke, L. Schultz, J. Wecker, and M. Katter, *Appl. Phys. Lett.*, *57*, 2853 (1990).
33. C. Kuhrt, L. Schultz, J. Wecker, K. Schnitzke, and M. Katter, to be published.
34. J.M.D. Coey, Hong Sun, Y. Otani, and D.P.F. Hurley, *J. Magn. Mater.*, *98*, 76 (1991).
35. M. Katter, J. Wecker, C. Kuhrt, L. Schultz, and R. Grössinger, *J. Magn. Mater.*, in print.